Research Article

Joao Carlos Monge, Jose Luis Mantari*, Melchor Nicolas Llosa, Miguel Angel Hinostroza

A size-dependent 3D solution of functionally graded shallow nanoshells

https://doi.org/10.1515/cls-2022-0215
received June 09, 2023; accepted August 27, 2023

Abstract: An unavailable semi-analytical non-local 3D solution for functionally graded nanoshells with constant radii of curvature is presented. The small length scale effect is included in Eringen's nonlocal elasticity theory. The constitutive and equilibrium equations are written in terms of curvilinear orthogonal coordinates systems which are only valid for spherical and cylindrical shells, and rectangular plates. The stresses and displacements are assumed in terms of the Navier method which is applicable for simply supported structures. The derivatives in terms of thickness are approximated by the differential quadrature method (DQM). The thickness domain is discretized by the Chebyshev–Gauss–Lobatto grid distribution. Lagrange interpolation polynomials are considered as the basis function for DQM. The correct free surface boundary condition for out-of-plane stresses is considered. Several problems of isotropic and functionally graded shells subjected to different types of loads are analyzed. The results are compared with other three-dimensional solutions and higher-order theories. It is important to emphasize that the radii of curvature are crucial at nanoscale, so it should be considered in the design of nanodevices.

Keywords: nanoshell, functionally graded material, Eringen's nonlocal elasticity theory, equilibrium equations

1 Introduction

Nanotechnology is applied in sensors, actuators, micro- and nano-electromechanical system, and atomic force microscope, and its components use different small-scale structures such as beams, plates, and shells [1]. The nanostructures can be studied by three different methods: quantum mechanics approach by solving the Schrödinger equations, molecular dynamics in which the interaction between atoms and molecules is computer simulated, and non-classical continuum mechanics (NCCM) [2]. The first two methods described incurred a higher computational cost compared to NCCM, so researchers have made valiant efforts and modifications to classical mechanics theories to incorporate the small-scale effect of the material and structure. NCCM can be classified into three different theories which are: strain gradient family, microcontinuum, and nonlocal elastic theories [1]. The strain gradient family can be divided into modified strain gradient theory [3,4] and modified couple stress [5,6]. Microcontinuum is classified into micropolar [7,8], microstretch [9], and micromorphic [10]. Nonlocal elastic theories were developed by Eringen [11–13] and were originally formulated in terms of an integral form and then reformulated to a differential form by introducing a Laplacian operator. Scientists have used the differential form of nonlocal theories due to its simplicity and easy extension for beams, plates, and shells. An extensive review of nonlocal theories for shells, plates, beam, frames, and rods was provided by Shariati *et al.* [14].

A survey on the topic reveals that several researchers have made a great contribution to the field of nonlocal theories. For example, Ansari and Rouhi [15] employed a nonlocal Flugge shell model to study the stability characteristics of single-walled carbon nanotubes under the action of axial load. Ritz method with different hyperbolic functions was utilized for evaluating different boundary conditions. Kananipour [16] investigated the static analysis of rectangular nanoplates subjected to discontinuous loads and different boundary conditions by differential quadrature method (DQM) in the framework of Kirchhoff and Mindlin plate theories. Srividhya *et al.* [17] developed a nonlocal nonlinear analysis of functionally graded plates subjected to static loads. The model was based on a higher order shear deformation theory (HSDT) and Von Karman nonlinear strains. Phung-Van *et al.* [18] employed a polynomial HSDT with five unknowns to study the free vibration and bending analysis of functionally

*** Corresponding author: Jose Luis Mantari,** Department of Science, Universidad de Ingenieria y Tecnologia - UTEC, Jr. Medrano Silva 165, Barranco, Lima, Peru; Postgraduate School, National University of Engineering, Av. Túpac Amaru 210, Rimac, Lima, Peru, e-mail: jmantari@utec.edu.pe, tel: +51 964358966
Joao Carlos Monge, Melchor Nicolas Llosa: Faculty of Physics, National University of San Marcos, Av. Carlos German Amezaga 375, Cercado de Lima, Lima, Peru
Miguel Angel Hinostroza: Faculty of Mechanical Engineering, National University of Engineering, Av. Túpac Amaru 210, Rimac, Lima, Peru

graded carbon nano-reinforced composite nanoplates. Isogeometric analysis was employed to approximate the derivatives of the general equations from a weak-form perspective.

Thai *et al.* [19] proposed a simple beam theory with one unknown to study the static response and free vibration of isotropic nanobeams. Analytical solutions were derived, and more accurate results than Euler–Bernoulli were obtained. Results were comparable with Timoshenko's beam theory. Jape and Sayyad [20] applied a hyperbolic nonlocal theory for the study of functionally graded nanobeams under uniform loads. The solutions are derived in terms of Navier's approach. Karami *et al.* [21] implemented the nonlocal strain gradient elasticity theory for the study of wave dispersion in anisotropic doubly-curved nanoshells employing a modified HSDT with 7 unknowns. Arefi and Zenkour [22] evaluated the free vibration analysis of sandwich nanoplates resting on Visco-Pasternak's foundation with an elastic nano core and two piezo-electromagnetic face sheets as sensors and actors. Mematollahi *et al.* [23] employed the classic plate theory for analyzing the free vibration of thin nanoplates involved in a thermal environment. The governing equations were obtained in terms of a higher-order nonlocal strain gradient theory and Navier' closed-form solution was employed. Arefi [24] studied the nonlocal electro-elastic bending of a doubly curved nanoshell resting on the Winkler–Pasternak foundation and subjected to transverse loading and voltage. The electric potential was assumed as a linear and cosine function combination, and the displacement field was approximated as the first-order shear deformation theory.

Ansari *et al.* [25] implement the Donnel shell theory for evaluating the free vibration of double-walled carbon nanotubes using a nonlocal elastic shell model. Van der Waals interactions between the inner and outer nanotubes were considered. The numerical solutions were given in terms of radial interpolation approximation in the framework of the DQM. Sahmani and Fattahi [26] utilized an HSDT for the study of the nonlocal nonlinear buckling and postbuckling response of temperature-dependent functionally graded carbon nanotube-reinforced composite shells under a combination of axial compression load and through-thickness heat conduction. She *et al.* [27] studied the free vibration of porous nanotubes which were assumed as functionally graded and vary continuously along the radial direction. The effects of nonlocal, strain gradient parameter, temperature variations, porosity volume fraction, and material variation were discussed.

Şimşek and Yurtcu [28] examined bending and buckling of a functionally graded nanobeam based on the Timoshenko and Euler–Bernoulli beam theory. The effect of nonlocal parameters, aspect ratio, and material constitution were discussed. Karami *et al.* [29] presented a simple model based on an HSDT for evaluating the static, stability, and free vibration of functionally graded carbon nanotubes-reinforced composite nanoplates resting on Winkler–Pasternak foundation. Thai *et al.* [30] employed the HSDT developed by Touratier [31] for studying bending, buckling, and free vibration of simply supported isotropic nanoplates. Ansari *et al.* [32] incorporated the classical Mindlin plate theory for the free vibration of single-layered graphene sheets. The boundary conditions were considered as simply supported and clamped, and the semi-analytical DQM was used for calculating the natural frequencies. The results were matched with molecular dynamic simulations to derive the approximate values of nonlocal parameters. Janghorban [33] employed an HSDT for investigating the characteristics and length parameters of the bending of functionally graded rectangular plates. Shahrbabaki [34] employed trigonometric series approximation functions in conjunction with the Galerkin approach to analyze 3D natural frequencies of nanoplates with different boundary conditions.

Curved structures are modeled by shell theories which can be derived in a two-dimensional (2D) and three-dimensional (3D) perspective. The 2D theories are developed in terms of unknown variables which are related to the mid-surface of the shell panel and expansion functions toward the thickness direction of the shell. The 3D solutions [35–42] can be derived in terms of finite elements which are implemented in commercial software; however, for simple geometries, limited boundary conditions, and orthotropic laminated structures some semi-analytical and analytical methods can be formulated. The governing equations for the 3D bending of shallow shell structures have variable coefficients which depend on the thickness direction. So, the solution requires different numerical methods such as finite difference [43], radial basis functions [44,45], sampling surfaces [46,47], discrete singular convolution [48,49], and DQM [50]. The last method described was formulated by Bellman and Casti [51], and several applications can be read in the review by Bert and Malik [52].

In this article, an available non-local semi-analytical 3D solution for bending of simply supported shallow nanoshells subjected to mechanical load is presented. The constitutive equations are based on Eringen's nonlocal theory. The equilibrium equations written in curvilinear coordinates are employed for the solutions. The system of nine equations is solved by the use of Navier-type solutions for stresses and displacements along with DQM for discretizing the thickness direction in terms of Chebyshev–Gauss–Lobatto grid distribution. Lagrange polynomials are employed as the basis function for DQM. The method is validated with other solutions and cases provided in the literature. Remarkably,

it is found that the radii of curvature in crucial at the nanoscale, so it should be considered in the design of nanodevices.

2 Three-dimensional solution for nanoshells

An innovative procedure to obtain a semi-analytical three-dimensional solution for the bending analysis of simply supported shallow nanoshells subjected to mechanical pressure is presented in this article for the first time. The nonlocal effect for stresses is included in the study of the constitutive equations. The presented model is only valid for spherical, cylindrical panels, and rectangular plates. A shell panel is described in terms of orthogonal curvilinear coordinates (α, β, z), and the representation for a spherical shell panel is shown in Figure 1. The length of the shell is denoted as "a," and the width is represented as "b," The radii of curvature "R_α" and "R_β" are considered as constant among the midsurface "Ω_k" The global thickness of the shell is denoted as "h."

2.1 Linear strains relations, constitutive equations, and equilibrium equations

The linear strain relations for shallow shell panels were reported and derived in classical textbooks [53–56], and they are described in what follows:

$$\begin{bmatrix} \varepsilon_{\alpha\alpha} \\ \varepsilon_{\beta\beta} \\ \gamma_{\alpha\beta} \\ \gamma_{\alpha z} \\ \gamma_{\beta z} \\ \varepsilon_{zz} \end{bmatrix} = \begin{bmatrix} \frac{1}{H_\alpha}\frac{\partial}{\partial\alpha} & 0 & \frac{1}{H_\alpha R_\alpha} \\ 0 & \frac{1}{H_\beta}\frac{\partial}{\partial\beta} & \frac{1}{H_\beta R_\beta} \\ \frac{1}{H_\beta}\frac{\partial}{\partial\beta} & \frac{1}{H_\alpha}\frac{\partial}{\partial\alpha} & 0 \\ \frac{\partial}{\partial z} - \frac{1}{H_\alpha R_\alpha} & 0 & \frac{1}{H_\alpha}\frac{\partial}{\partial\alpha} \\ 0 & \frac{\partial}{\partial z} - \frac{1}{H_\beta R_\beta} & \frac{1}{H_\beta}\frac{\partial}{\partial\beta} \\ 0 & 0 & \frac{\partial}{\partial z} \end{bmatrix} \begin{bmatrix} u \\ v \\ w \end{bmatrix}. \tag{1}$$

The metric parameters are related to the radii of curvature, and the thickness coordinate of the panel and are written as

$$\begin{aligned} H_\alpha &= 1 + \frac{z}{R_\alpha} \\ H_\beta &= 1 + \frac{z}{R_\beta}. \end{aligned} \tag{2}$$

The metric coefficients "H_α" and "H_β" establish the type of geometry to be considered. If one of the radii of curvature

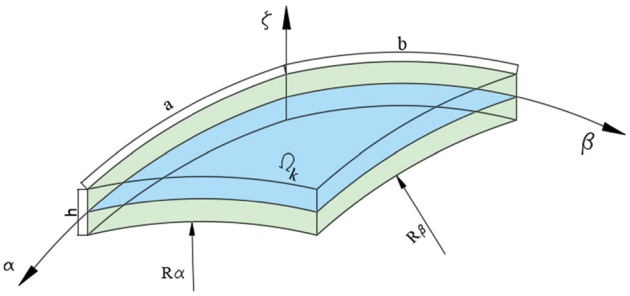

Figure 1: The representation of a doubly curved shell.

is considered infinite, the structure has a cylindrical geometry. A rectangular plate is prescribed when both radii of curvatures are infinite. So, these general equations can be applied to spherical, cylindrical, and rectangular plates by degenerating the radii of curvature.

The constitutive equations are used for calculating the stresses, which are related to the linear strain as follows:

$$\begin{aligned} (1 - \mu\nabla^2)\begin{bmatrix} \sigma_{\alpha\alpha} \\ \sigma_{\beta\beta} \\ \tau_{\alpha\beta} \\ \tau_{\alpha z} \\ \tau_{\beta z} \\ \sigma_{zz} \end{bmatrix} &= \begin{bmatrix} C_{11} & C_{12} & 0 & 0 & 0 & C_{13} \\ C_{12} & C_{22} & 0 & 0 & 0 & C_{23} \\ 0 & 0 & C_{66} & 0 & 0 & 0 \\ 0 & 0 & 0 & C_{55} & 0 & 0 \\ 0 & 0 & 0 & 0 & C_{44} & 0 \\ C_{13} & C_{23} & 0 & 0 & 0 & C_{33} \end{bmatrix} \begin{bmatrix} \varepsilon_{\alpha\alpha} \\ \varepsilon_{\beta\beta} \\ \gamma_{\alpha\beta} \\ \gamma_{\alpha z} \\ \gamma_{\beta z} \\ \varepsilon_{zz} \end{bmatrix} \\ &= \begin{bmatrix} \sigma_{\alpha\alpha}^{\mathrm{NL}} \\ \sigma_{\alpha\alpha}^{\mathrm{NL}} \\ \tau_{\alpha\beta}^{\mathrm{NL}} \\ \tau_{\alpha z}^{\mathrm{NL}} \\ \tau_{\beta z}^{\mathrm{NL}} \\ \sigma_{zz}^{\mathrm{NL}} \end{bmatrix}. \end{aligned} \tag{3}$$

The parameter μ is considered as a nanometric factor, and its numerical value is considered as $0 \le \mu \le 4 \quad \mathrm{nm}^2$ [57]. The nonlocal stresses are represented as $[\sigma_{\alpha\alpha}^{\mathrm{NL}}, \sigma_{\beta\beta}^{\mathrm{NL}}, \sigma_{zz}^{\mathrm{NL}}, \tau_{\alpha\beta}^{\mathrm{NL}}, \tau_{\alpha z}^{\mathrm{NL}}, \tau_{\beta z}^{\mathrm{NL}}]$. The Laplacian operator ∇^2 is written in terms of the midsurface coordinates and is expressed as:

$$\nabla^2 = \frac{1}{H_\alpha{}^2}\frac{\partial^2}{\partial\alpha^2} + \frac{1}{H_\beta{}^2}\frac{\partial^2}{\partial\beta^2}. \tag{4}$$

The stiffness coefficients C_{ij} can be calculated in the following manner:

$$\begin{aligned} C_{11} = C_{22} = C_{33} &= \frac{(1-\nu)E}{(1+\nu)(1-2\nu)} \\ C_{12} = C_{13} = C_{23} &= \frac{\nu E}{(1+\nu)(1-2\nu)} \\ C_{44} = C_{55} = C_{66} &= \frac{E}{2(1+\nu)}. \end{aligned} \tag{5}$$

The equilibrium equations are developed in orthogonal curvilinear (α, β, z) and are valid for doubly curved shell panels with constant curvature. Several applications can be found in refs. [58–61]. The equilibrium equations are reported as follows:

$$\begin{aligned}
&H_\beta\frac{\partial\sigma_{\alpha\alpha}}{\partial\alpha}+H_\alpha\frac{\partial\tau_{\alpha\beta}}{\partial\beta}+H_\alpha H_\beta\frac{\partial\tau_{\alpha z}}{\partial z}+\left(\frac{2H_\beta}{R_\alpha}+\frac{H_\alpha}{R_\beta}\right)\tau_{\alpha z}=0\\
&H_\beta\frac{\partial\tau_{\alpha\beta}}{\partial\alpha}+H_\alpha\frac{\partial\sigma_{\beta\beta}}{\partial\beta}+H_\alpha H_\beta\frac{\partial\tau_{\beta z}}{\partial z}+\left(\frac{2H_\alpha}{R_\beta}+\frac{H_\beta}{R_\alpha}\right)\tau_{\beta z}=0\\
&H_\beta\frac{\partial\tau_{\alpha z}}{\partial\alpha}+H_\alpha\frac{\partial\tau_{\beta z}}{\partial\beta}+H_\alpha H_\beta\frac{\partial\sigma_{zz}}{\partial z}-\frac{H_\beta}{R_\alpha}\sigma_{\alpha\alpha}-\frac{H_\alpha}{R_\beta}\sigma_{\beta\beta}\\
&\quad+\left(\frac{H_\beta}{R_\alpha}+\frac{H_\alpha}{R_\beta}\right)\sigma_{zz}=0.
\end{aligned}\tag{6}$$

The equilibrium equations are derived from the Principle of Virtual Displacement and the complete derivation can be seen in ref. [58].

2.2 3D bending solutions of nanoshells

Closed-form summations of trigonometric harmonics are employed for solving the partial differential equations for the midsurface coordinates "α" and "β. " The stresses and displacements are written in terms of the Fourier series:

$$\begin{aligned}
&\{w,\sigma_{\alpha\alpha},\sigma_{\beta\beta},\sigma_{zz}\}\\
&\quad=\sum_{m=1}^{\infty}\sum_{n=1}^{\infty}\{w(z),\sigma_{\alpha\alpha}(z),\sigma_{\beta\beta}(z),\sigma_{zz}(z)\}\sin(\bar\alpha\alpha)\sin(\bar\beta\beta)\\
&\{u,\tau_{\alpha z}\}=\sum_{m=1}^{\infty}\sum_{n=1}^{\infty}\{u(z),\tau_{\alpha z}(z)\}\cos(\bar\alpha\alpha)\sin(\bar\beta\beta)\\
&\{v,\tau_{\beta z}\}=\sum_{m=1}^{\infty}\sum_{n=1}^{\infty}\{v(z),\tau_{\beta z}(z)\}\sin(\bar\alpha\alpha)\cos(\bar\beta\beta)\\
&\{\tau_{\alpha\beta}\}=\sum_{m=1}^{\infty}\sum_{n=1}^{\infty}\{\tau_{\alpha\beta}(z)\}\cos(\bar\alpha\alpha)\cos(\bar\beta\beta)\\
&\bar\alpha=\frac{r\pi}{a},\bar\beta=\frac{s\pi}{b}.
\end{aligned}\tag{7}$$

These harmonic summations can only be applied for shells with constant radii of curvature and for panels in which edge boundary conditions are considered as simply supported. The wave numbers are denoted as "r" and "s." The amplitudes for stresses are named "$\sigma_{\alpha\alpha}(z), \sigma_{\beta\beta}(z), \sigma_{zz}(z), \tau_{\alpha z}(z), \tau_{\beta z}(z), \tau_{\alpha\beta}(z)$" and for displacement "$u(z), v(z), w(z)$. " Fourier series are replaced in the equilibrium and constitute equations, and the following equations are formed:

$$\begin{aligned}
&\left(1+\frac{\mu\bar\alpha^2}{H_\alpha{}^2}+\frac{\mu\bar\beta^2}{H_\beta{}^2}\right)\sigma_{\alpha\alpha}-C_{13}\frac{\partial w}{\partial z}-\left(\frac{C_{11}}{H_\alpha R_\alpha}+\frac{C_{12}}{H_\beta R_\beta}\right)w\\
&\quad+\frac{\bar\alpha C_{11}}{H_\alpha}u+\frac{\bar\beta C_{12}}{H_\beta}=0\\
&\left(1+\frac{\mu\bar\alpha^2}{H_\alpha{}^2}+\frac{\mu\bar\beta^2}{H_\beta{}^2}\right)\sigma_{\beta\beta}-C_{23}\frac{\partial w}{\partial z}-\left(\frac{C_{12}}{H_\alpha R_\alpha}+\frac{C_{22}}{H_\beta R_\beta}\right)w\\
&\quad+\frac{\bar\alpha C_{12}}{H_\alpha}u+\frac{\bar\beta C_{22}}{H_\beta}=0\\
&\left(1+\frac{\mu\bar\alpha^2}{H_\alpha{}^2}+\frac{\mu\bar\beta^2}{H_\beta{}^2}\right)\sigma_{zz}-C_{33}\frac{\partial w}{\partial z}-\left(\frac{C_{13}}{H_\alpha R_\alpha}+\frac{C_{23}}{H_\beta R_\beta}\right)w\\
&\quad+\frac{\bar\alpha C_{13}}{H_\alpha}u+\frac{\bar\beta C_{23}}{H_\beta}=0\\
&\left(1+\frac{\mu\bar\alpha^2}{H_\alpha{}^2}+\frac{\mu\bar\beta^2}{H_\beta{}^2}\right)\tau_{\alpha\beta}-\frac{C_{66}\bar\beta}{H_\beta}u-\frac{C_{66}\bar\alpha}{H_\alpha}v=0\\
&\left(1+\frac{\mu\bar\alpha^2}{H_\alpha{}^2}+\frac{\mu\bar\beta^2}{H_\beta{}^2}\right)\tau_{\alpha z}-C_{55}\frac{\partial u}{\partial z}+\frac{C_{55}}{H_\alpha R_\alpha}u-\frac{\bar\alpha C_{55}}{H_\alpha}w=0\\
&\left(1+\frac{\mu\bar\alpha^2}{H_\alpha{}^2}+\frac{\mu\bar\beta^2}{H_\beta{}^2}\right)\tau_{\beta z}-C_{44}\frac{\partial v}{\partial z}+\frac{C_{44}}{H_\beta R_\beta}v-\frac{\bar\beta C_{44}}{H_\beta}w=0\\
&\frac{\partial\tau_{\alpha z}}{\partial z}+\left(\frac{2}{H_\alpha R_\alpha}+\frac{1}{H_\beta R_\beta}\right)\tau_{\alpha z}-\frac{\bar\beta}{H_\beta}\tau_{\alpha\beta}+\frac{\bar\alpha}{H_\alpha}\sigma_{\alpha\alpha}=0\\
&\frac{\partial\tau_{\beta z}}{\partial z}+\left(\frac{1}{H_\alpha R_\alpha}+\frac{2}{H_\beta R_\beta}\right)\tau_{\alpha z}-\frac{\bar\alpha}{H_\alpha}\tau_{\alpha\beta}+\frac{\bar\beta}{H_\beta}\sigma_{\beta\beta}=0\\
&\frac{\partial\sigma_{zz}}{\partial z}+\left(\frac{1}{H_\alpha R_\alpha}+\frac{1}{H_\beta R_\beta}\right)\sigma_{zz}-\frac{\bar\alpha}{H_\alpha}\tau_{\alpha z}-\frac{\bar\beta}{H_\beta}\tau_{\beta z}-\frac{\sigma_{\alpha\alpha}}{H_\alpha R_\alpha}\\
&\quad-\frac{\sigma_{\beta\beta}}{H_\beta R_\beta}=0.
\end{aligned}\tag{8}$$

The coefficients of the system of nine differential equations are considered as variable due to the metric coefficients and depend on the thickness coordinates. No analytical solutions can be derived because of the thickness dependence coefficients. So, a semi-analytical solution is reported based on the so-called DQM. This numerical procedure permits calculation of the derivative of a stress or displacement by a linear sum of each variable (stress or displacement) evaluated in a certain grid point distribution. The mathematical expression for DQM is reported as follows:

$$\left.\frac{\mathrm{d}f}{\mathrm{d}z_k}\right|_{z_k=z_i}=\sum_{j=1}^{T}a_{ij}f(z_j),\ i=1,2,...,T.\tag{9}$$

The weighted coefficients are denoted as a_{ij}. There are different manners of calculating a_{ij}, and several procedures were reported in the survey by Tornabene *et al.* [62]. The basis function employed is the Lagrange interpolation polynomials (LIP) [63] and are reported as follows:

$$L(z_j) = \prod_{i=1, i\neq j}^{I_T} (z_j - z_i). \tag{10}$$

The principal advantage of LIP is that an arbitrary grid distribution can be applied. A recursive formula is applied for the weighted coefficients [63], and its formulation for the first- and second-order derivative can be expressed as:

$$\begin{aligned} a_{ij}^{(1)} &= \frac{L^{(1)}(z_j)}{(z_i - z_j)L(z_j)}, i, j = 1, 2, ..., I_T, i \neq j \\ a_{ij}^{(2)} &= 2\left(a_{ii}^{(1)} a_{ij}^{(1)} - \frac{a_{ij}^{(1)}}{(z_i - z_j)}\right), i, j = 1, 2, ..., I_T, i \neq j \\ a_{ii}^{(n)} &= -\sum_{j=1, j\neq i}^{I_T} a_{ij}^{(n)}, i, j = 1, 2, ..., I_T, i = j, n = 1, 2. \end{aligned} \tag{11}$$

The thickness of the shell panel is discretized in terms of Chebyshev–Gauss–Lobatto grid distribution:

$$z_i = \frac{(-h)}{2}\left(\cos\left(\frac{i-1}{I_T - 1}\pi\right)\right), i = 1, 2, ..., I_T. \tag{12}$$

The traction conditions of the out-plane stress for the bottom (b) and top (t) are expressed as:

$$\begin{aligned} \sigma_{zz}^{(t)} &= P_{mn}, \sigma_{zz}^{(b)} = 0 \\ \tau_{\alpha z}^{(t)} &= \tau_{\alpha z}^{(b)} = 0 \\ \tau_{\beta z}^{(t)} &= \tau_{\beta z}^{(b)} = 0. \end{aligned} \tag{13}$$

It is assumed that the shell panel is subjected to a transverse load at the top of the panel, and it can be written in terms of harmonics:

$$p_{z_s}^k = \sum_{r,s} P_{rs}^k \sin\left(\frac{r\pi}{a}\alpha\right)\sin\left(\frac{s\pi}{b}\beta\right). \tag{14}$$

The coefficient of the mechanical load for a uniformly distributed load is expressed as:

$$P_{rs}^k = \begin{cases} \dfrac{16P_z}{\pi^2 rs}, \text{for} \quad \{r, s\} = 1, 3, 5, 7, ... \\ 0, \text{for} \quad \{r, s\} = 2, 4, 6, 8, ... \end{cases} \tag{15}$$

The implementation of weighted coefficients, the traction boundary conditions, and governing equations for shallow nanoshells subjected to a mechanical load are developed in MATLAB code.

3 Results

The target of this article is to perform the static analysis of nanoshells with constant curvature based on Eringen's nonlocal theory. The shallow shell panels are subjected to bisinusoidal and uniformly distributed loads. The first case problem was reported in the article by Wu and Li [57], who studied an isotropic nanoplate subjected to a bisinusoidal load. The second case problem was reported by Nguyen *et al.* [64], and it is about functionally graded nanoplates subjected to uniformly distributed load. The authors modeled the properties by the Mori and Tanaka scheme [65]. Overall, these problems can be used for extending the case to doubly curved panels and cylindrical panels.

The transverse displacement w and normal nonlocal stresses $\sigma_{\alpha\alpha}^{\mathrm{NL}}, \sigma_{\beta\beta}^{\mathrm{NL}}, \sigma_{zz}^{\mathrm{NL}}$ are evaluated at $(a/2, b/2, z)$. The in-plane shear stress $\tau_{\alpha\beta}^{\mathrm{NL}}$ is calculated at $(0,0, z)$. The in-plane displacement u and shear stress $\tau_{\alpha z}^{\mathrm{NL}}$ are estimated at $(0, b/2, z)$. The displacement v and out-of-plane stress $\tau_{\beta z}^{\mathrm{NL}}$ are assessed at $(a/2,0, z)$.

3.1 Isotropic shells subjected to a bisinusoidal load

A simply supported isotropic plate is subjected to a bisinusoidal load. The plate is considered as a single-layered graphene sheet whose properties are $E = 1.02$ TPa, $\nu = 0.16$ and the thickness of the plate is $h = 0.34$ nm, the panel key ratios are length-to-thickness ratio (a/h) and length aspect ratios (b/a). The normalizations of stresses and displacements are given by the following formula:

$$\begin{aligned} (\bar{u}, \bar{w}) &= \left(\frac{uEh^2}{Pa^3}, \frac{-100wEh^3}{Pa^4}\right), \\ (\bar{\sigma}_{\alpha\alpha}^{\mathrm{NL}}, \bar{\tau}_{\alpha\beta}^{\mathrm{NL}}, \bar{\tau}_{\alpha z}^{\mathrm{NL}}) &= \left(\frac{\sigma_{\alpha\alpha}^{\mathrm{NL}} h^2}{Pa^2}, \frac{\tau_{\alpha\beta}^{\mathrm{NL}} h^2}{Pa^2}, \frac{\tau_{\alpha z}^{\mathrm{NL}} h}{Pa}\right) \end{aligned} \tag{16}$$

The numerical normalized results for displacements $(\bar{u}, \bar{w})$ and nonlocal stresses $(\bar{\sigma}_{\alpha\alpha}^{\mathrm{NL}}, \bar{\tau}_{\alpha\beta}^{\mathrm{NL}}, \bar{\tau}_{\alpha z}^{\mathrm{NL}})$ are presented in Table 1. In this case, the thickness of the plate is discretized into $I_T = 9$ points. It is demonstrated that the results were the same as the 3D referential solution proposed by Wu and Li [57] employing the perturbation method. Then, the problem is extended to spherical and cylindrical panels by considering the radius-to-size (R/a) ratio. A thickness ratio of $a/h = 10$ is considered. For a

Table 1: Results of an isotropic plate subjected to bisinusoidal load

a/h	b/a	Theory	$\mu = 0$	$\mu = 0.5$	$\mu = 1$	$\mu = 1.5$	$\mu = 2$
10	1	$\bar{u}(h/2)$ [57]	0.0472	0.0874	0.1277	0.168	0.2083
		$\bar{u}(h/2)$ [Present]	0.0472	0.0874	0.1277	0.168	0.2083
		$\bar{w}(0)$ [57]	3.1331	5.8081	8.483	11.158	13.833
		$\bar{w}(0)$ [Present]	3.1331	5.8081	8.483	11.158	13.833
		$\bar{\sigma}^{\mathrm{NL}}_{\alpha\alpha}(h/2)$ [57]	0.1774	0.3289	0.4804	0.6319	−0.7833
		$\bar{\sigma}^{\mathrm{NL}}_{\alpha\alpha}(h/2)$ [Present]	0.1774	0.3289	0.4804	0.6319	0.7833
		$\bar{\tau}^{\mathrm{NL}}_{\alpha\beta}(h/2)$ [57]	−0.1285	−0.2382	−0.3479	−0.4575	−0.5672
		$\bar{\tau}^{\mathrm{NL}}_{\alpha\beta}(h/2)$ [Present]	−0.1285	−0.2382	−0.3479	−0.4575	−0.5672
		$\bar{\tau}^{\mathrm{NL}}_{\alpha z}(0)$ [57]	−0.2383	−0.4418	−0.6453	−0.8488	−1.0523
		$\bar{\tau}^{\mathrm{NL}}_{\alpha z}(0)$ [Present]	−0.2383	−0.4418	−0.6453	−0.8488	−1.0523
	2	$\bar{u}(h/2)$ [57]	0.1207	0.1851	0.2495	0.314	0.3784
		$\bar{u}(h/2)$ [Present]	0.1207	0.1851	0.2495	0.314	0.3784
		$\bar{w}(0)$ [57]	7.8941	12.1065	16.3189	20.5313	24.7436
		$\bar{w}(0)$ [Present]	7.8941	12.1065	16.3189	20.5313	24.7436
		$\bar{\sigma}^{\mathrm{NL}}_{\alpha\alpha}(h/2)$ [57]	0.4063	0.6231	0.8398	1.0566	1.2734
		$\bar{\sigma}^{\mathrm{NL}}_{\alpha\alpha}(h/2)$ [Present]	0.4063	0.6231	0.8398	1.0566	1.2734
		$\bar{\tau}^{\mathrm{NL}}_{\alpha\beta}(h/2)$ [57]	−0.1641	−0.2516	−0.3392	−0.4267	−0.5143
		$\bar{\tau}^{\mathrm{NL}}_{\alpha\beta}(h/2)$ [Present]	−0.1641	−0.2516	−0.3392	−0.4267	−0.5143
		$\bar{\tau}^{\mathrm{NL}}_{\alpha z}(0)$ [57]	−0.3816	−0.5852	−0.7888	−0.9924	−1.196
		$\bar{\tau}^{\mathrm{NL}}_{\alpha z}(0)$ [Present]	−0.3816	−0.5852	−0.7888	−0.9924	−1.196
20	1	$\bar{u}(h/2)$ [57]	0.0471	0.0572	0.0673	0.0773	0.0874
		$\bar{u}(h/2)$ [Present]	0.0471	0.0572	0.0673	0.0773	0.0874
		$\bar{w}(0)$ [57]	3.0341	3.6817	4.3293	4.9769	5.6245
		$\bar{w}(0)$ [Present]	3.0341	3.6817	4.3293	4.9769	5.6245
		$\bar{\sigma}^{\mathrm{NL}}_{\alpha\alpha}(h/2)$ [57]	0.1766	0.2143	0.252	0.2897	0.3274
		$\bar{\sigma}^{\mathrm{NL}}_{\alpha\alpha}(h/2)$ [Present]	0.1766	0.2143	0.252	0.2897	0.3274
		$\bar{\tau}^{\mathrm{NL}}_{\alpha\beta}(h/2)$ [57]	−0.1279	−0.1552	−0.1825	−0.2098	−0.237
		$\bar{\tau}^{\mathrm{NL}}_{\alpha\beta}(h/2)$ [Present]	−0.1279	−0.1552	−0.1825	−0.2098	−0.237
		$\bar{\tau}^{\mathrm{NL}}_{\alpha z}(0)$ [57]	−0.2386	−0.2896	−0.3405	−0.3914	−0.4424
		$\bar{\tau}^{\mathrm{NL}}_{\alpha z}(0)$ [Present]	−0.2386	−0.2896	−0.3405	−0.3914	−0.4424
	2	$\bar{u}(h/2)$ [57]	0.1207	0.1368	0.1529	0.169	0.1851
		$\bar{u}(h/2)$ [Present]	0.1207	0.1368	0.1529	0.169	0.1851
		$\bar{w}(0)$ [57]	7.7354	8.7674	9.7993	10.8312	11.8631
		$\bar{w}(0)$ [Presented]	7.7354	8.7674	9.7993	10.8312	11.8631
		$\bar{\sigma}^{\mathrm{NL}}_{\alpha\alpha}(h/2)$ [57]	0.4051	0.4591	0.5131	0.5672	0.6212
		$\bar{\sigma}^{\mathrm{NL}}_{\alpha\alpha}(h/2)$ [Present]	0.4051	0.4591	0.5131	0.5672	0.6212
		$\bar{\tau}^{\mathrm{NL}}_{\alpha\beta}(h/2)$ [57]	−0.1636	−0.1854	−0.2072	−0.229	−0.2509
		$\bar{\tau}^{\mathrm{NL}}_{\alpha\beta}(h/2)$ [Present]	−0.1636	−0.1854	−0.2072	−0.229	−0.2509
		$\bar{\tau}^{\mathrm{NL}}_{\alpha z}(0)$ [57]	−0.3819	−0.4328	−0.4838	−0.5347	−0.5856
		$\bar{\tau}^{\mathrm{NL}}_{\alpha z}(0)$ [Present]	−0.3819	−0.4328	−0.4838	−0.5347	−0.5856

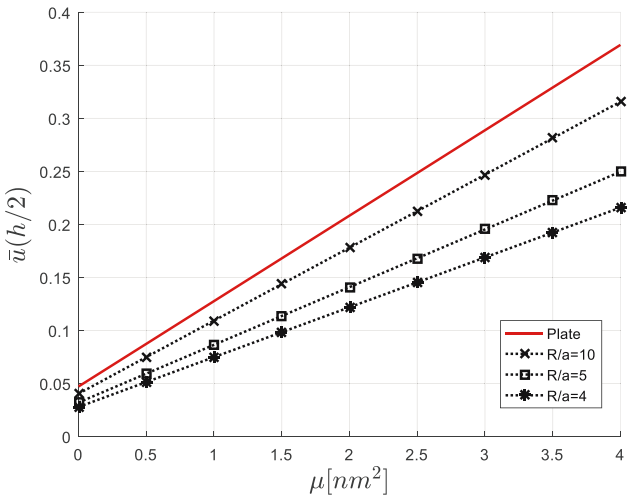

Figure 2: Normalized displacement $\bar{u}$ *vs* nonlocal factor for an isotropic spherical shell.

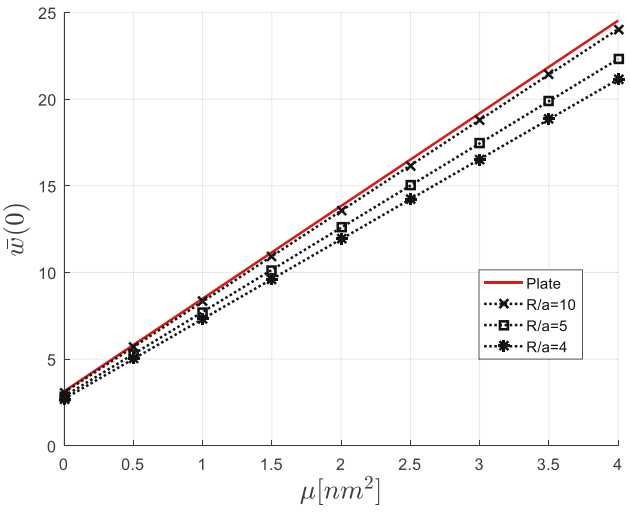

Figure 4: Normalized displacement $\bar{w}$ *vs* nonlocal factor for an isotropic spherical shell.

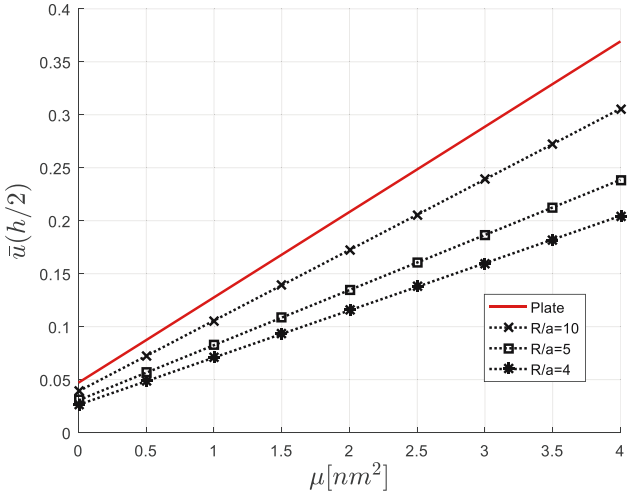

Figure 3: Normalized displacement $\bar{u}$ *vs* nonlocal factor for an isotropic cylindrical shell.

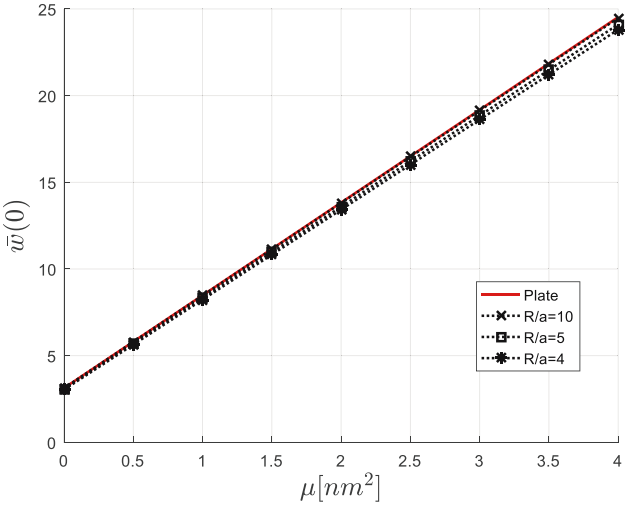

Figure 5: Normalized displacement $\bar{w}$ *vs* nonlocal factor for an isotropic cylindrical shell.

cylindrical panel, the radius R_β is equal to infinite. Figures 2 and 3 show the relationship between normalized deformation $\bar{u}$ and non-local parameters for a spherical and cylindrical panel, respectively. In the case of normalized deformation of shells, the same relation can be seen in Figures 4 and 5. The results demonstrated as the nonlocal parameter increased, the normalized deformation also increased. On the other hand, as the ratio (R/a) decreases, the normalized deformation also decreases. Interestingly, it is important to remark that the radii of curvature play a crucial role at the nanoscale and must be considered in future research activities for the proper design of nanodevices.

3.2 Functionally graded plate subjected to uniformly distributed load

A simply supported plate is subjected to a uniformly distributed load. The functionally graded mechanical properties are modeled by the Mori–Tanaka model as follows:

$$\frac{K_e - K_m}{K_c - K_m} = \frac{V_c}{1 + V_m \frac{K_c - K_m}{K_m + 4/3G_m}}$$
$$\frac{G_e - G_m}{G_c - G_m} = \frac{V_c}{1 + V_m \frac{G_c - G_m}{G_m + f_1}} \tag{17}$$
$$f_1 = \frac{G_m(9K_m + 8G_m)}{6(K_m + 2G_m)},$$

Table 2: Results of an isotropic plate subjected to uniform distributed load

p	Model	$a/h = 5$			$a/h = 10$			$a/h = 50$		
		$\mu = 0$	$\mu = 1$	$\mu = 4$	$\mu = 0$	$\mu = 1$	$\mu = 4$	$\mu = 0$	$\mu = 1$	$\mu = 4$
0	Nguyen et al. [64]	0.0902	0.1059	0.1529	0.0787	0.0928	0.1351	0.075	0.0886	0.1294
	Phung-Van *et al.* [18]	0.0903	0.1060	0.153	0.0787	0.0928	0.1351	0.075	0.0886	0.1294
	Present	0.0885	0.1039	0.1502	0.0783	0.0923	0.1344	0.075	0.0886	0.1293
1	Nguyen *et al.* [64]	0.2254	0.2646	0.3821	0.1977	0.2331	0.3393	0.1888	0.223	0.3256
	Phung-Van *et al.* [18]	0.2254	0.2646	0.3821	0.1977	0.2331	0.3394	0.1888	0.223	0.3256
	Present	0.2243	0.2634	0.3806	0.1974	0.2328	0.339	0.1888	0.223	0.3256
2	Nguyen *et al.* [64]	0.2723	0.3194	0.4606	0.2344	0.2763	0.4021	0.2222	0.2625	0.3834
	Phung-Van *et al.* [18]	0.2721	0.3192	0.4603	0.2344	0.2763	0.4021	0.2222	0.2625	0.3834
	Present	0.2714	0.3185	0.4596	0.2343	0.2762	0.4019	0.2222	0.2625	0.3833
5	Nguyen *et al.* [64]	0.3247	0.3804	0.5477	0.2730	0.3217	0.4678	0.2564	0.3028	0.4422
	Phung-Van *et al.* [18]	0.3246	0.3803	0.5474	0.2729	0.3217	0.4678	0.2564	0.3028	0.4422
	Present	0.3227	0.3782	0.5449	0.2726	0.3212	0.4672	0.2564	0.3028	0.4422
10	Nguyen *et al.* [64]	0.3620	0.4243	0.6109	0.3052	0.3597	0.5231	0.2869	0.339	0.495
	Phung-Van *et al.* [18]	0.3625	0.4247	0.6114	0.3053	0.3598	0.5233	0.2870	0.339	0.495
	Present	0.3594	0.4213	0.6071	0.3047	0.3591	0.5223	0.2870	0.339	0.495

where K and G are defined as the Bulk and shear modulus. The subscript "m" stands for metallic composition, and "c" is for the ceramic constitution. The volume fractions are considered as a function of the thickness direction and are considered by the following relation:

$$V_c = \left(\frac{1}{2} + \frac{z}{h}\right)^p, V_m = 1 - V_c. \tag{18}$$

The exponent of the ceramic volume fraction is given as "p." The elastic modulus and Poisson ratio for computing the stiffness coefficients (Eq. (5)) are calculated as:

$$E = \frac{9KG}{3K + G}, \nu = \frac{3K - 2G}{2(3K + G)}. \tag{19}$$

The properties of the metallic constitution are (E_m = 70 GPa, υ_m = 0.30)[Al] and for ceramic are (E_c = 380 GPa, υ_c = 0.30)[Al_2O_3]. The geometry of the plate is considered as $a = b$ = 10nm. The load is considered uniform distributed (Eq. (15)) and $r = s$ = 31 are considered as the index for the summation of harmonics. For this numerical example, the panel is discretized with I_T = 19. Phung-Van *et al.* [18] solve this problem by an HSDT and an isogeometric analysis. Nguyen *et al.* [64] employed an HSDT with four unknowns and isogeometric technique. The normalized transverse displacement is presented:

$$\bar{w} = \frac{100E_m h^3}{12(1 - \upsilon_m^2)Pa^4} w(a/2, b/2, 0). \tag{20}$$

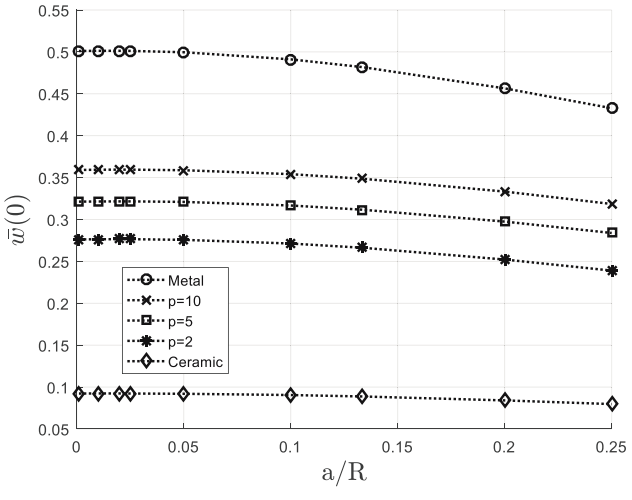

Figure 6: Normalized displacement $\bar{w}$ *vs* ratio a/R for a functionally graded spherical shell.

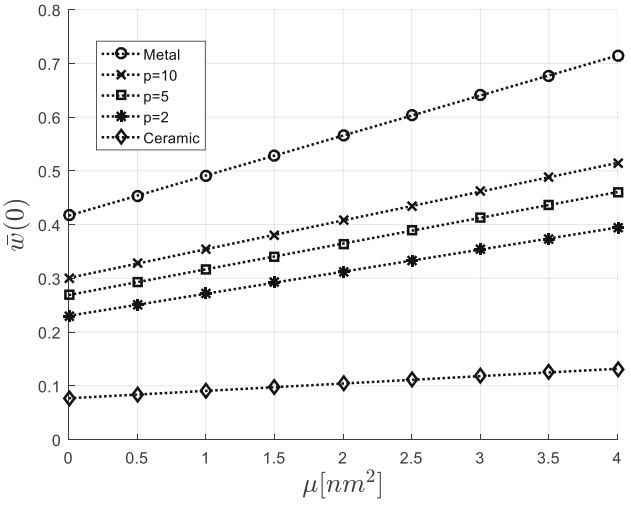

Figure 7: Normalized displacement $\bar{w}$ *vs* nonlocal factor for a functionally graded spherical shell.

The numerical results for transverse displacement are reported in Table 2. It is seen that for thin plates (a/h = 50), the results are in total concordance with the higher order theories. A slightly numerical difference is evidenced for thick (a/h = 5) and moderated thick plates (a/h = 10) between the presented model and 2D theories. In thick nanoplates, the capability of the 3D solution is evidenced.

A moderated thick spherical shell (a/h = 10) is considered for parametric analysis. Figure 6 shows the normalized centered transverse displacement as a function of a/R, considering a nonlocal parameter μ = 1nm^2. It is seen that as the exponent "p" increases, the normalized displacement also increases; as the ratio a/R increases, the normalized displacement decreases. A nonlinear relationship is evidenced, and the radii of curvature are crucial at nanoscale. Figure 7 shows the relationship between the transverse centered displacement and the nonlocal parameter "μ," considering a ratio of R/a = 10. It is demonstrated a linear correlation for the material exponent parameters considered. As the nonlocal parameter increases, the displacement increases. This pattern is kept for different radius-to-length ratios.

Overall, it is important to remark that is extremally important the influence of the radii of curvature on the bending response of nanoshells. Suppressively, as far as the author is concerned, there is no contribution in this field. Consequently, these problems can be considered as the referential solution for other numerical models.

Moreover, the present technique could be used to solve other problems such as clamped nanoplates by the use of the boundary discontinuous method. Currently, this method can be extended to more sophisticated structures such as functionally graded carbon-nanotubes-reinforced laminated composites [66] or graphene nanoplatelet reinforced composites [67]. Additionally, multilayered structures and complex shell structures can also be faced.

4 Conclusions

A smart semi-analytical solution for the bending of simply supported spherical, cylindrical, and rectangular nanostructures is presented. The nonlocal scale is considered by Eringen's nonlocal theory. The equilibrium equations are written in terms of curvilinear coordinates. The stresses and mechanical displacements are expressed in closed-form summations of harmonic for the midsurface of the plate and are discretized with the classic Chebyshev–Gauss–Lobatto. The governing equations are solved semi-analytical by the DQM, and Lagrange Interpolation polynomials are used as basis functions. The results are compared with 3D theories and 2D theories provided in the literature for isotropic and functionally graded rectangular plates subjected to bisinusoidal and uniform distributed load. Since remarkable results were obtained for plates, the case problems were extended for cylindrical and spherical panels. Remarkably, the influence of the radii of curvature on the bending response of nanoshells is significant, and it should be a strong topic of research since it is crucial in the design of nanodevices. Nanoshell problems are solved in a closed form in this article, so they can be considered benchmark nanoshell solutions for future works. Finally, the method can be extended for multilayered shells and for different functionally reinforced constitutive such as carbon nanotubes and graphene nanoplatelets.

Funding information: This article was written in the context of the project: "Desarrollo de un algoritmo autónomo y óptimo de mecánica computacional para un análisis de estructuras complejas impresa con tecnología 3D, utilizando inteligencia artificial y algoritmos genéticos" founded by CONCYTEC under the contract number N°060-2021-PROCIENCIA. The authors of this manuscript appreciate the financial support from the Peruvian Government.

Author contributions: All authors have accepted responsibility for the entire content of this manuscript and approved its submission.

Conflict of interest: The authors have no conflicts of interest to declare.

References

[1] Thai HT, Vo T, Nguyen TK, Seung-Eock K. A review of continuum mechanics models for size-dependent analysis of beams and plates. Compos Struct. 2017;177:196–219.
[2] Khoram MM, Hosseimi M, Shishesaz M. A concise review of nanoplates. J Comput Appl Mech. 2019;50(2):420–9.
[3] Thai CT, Ferreira AJM, Phung-Van P. Size dependent free vibration analysis of multilayered GPLRC microplates based on modified strain gradient theory. Compos B: Eng. 2019;169:174–88.
[4] Hajilak EZ, Pourghader J, Hashemabadi D, Bagh SF, Habibi M. Multilayer GPLRC composite cylindrical nanoshell using modified strain gradient theory. Mech Based Des Struct Mach. 2019;47(5):521–45.
[5] Asghari M, Rahaeifard M, Kahrobaiyan MH, Ahmadian MT. The modified couple stress functionally graded Timoshenko beam formulation. Mater Des. 2011;32:1435–43.
[6] Zare Jouneghani F, Babamoradi H, Dimitri R, Tornabene F. A modified couple stress elasticity for non-uniform composite laminated beams based on the Ritz formulation. Molecules. 2020;25(6):1404.

[7] Carrera E, Zozulya VV. Carrera unified formulation for the micropolar plates. Mech Adv Mater Struct. 2011;29(22):3163–86.
[8] Karttunen AT, Reddy JN, Romanoff J. Micropolar modeling approach for periodic sandwich beams. Compos Struct. 2018;185:656–64.
[9] Liu X, Hu G. Inclusion of microstretch continuum. Int J Eng Sci. 2004;42:849–60.
[10] Eringen AC. Compatibility conditions of the theory of micromorphic elastic solids. J Math Mech. 1969;19(6):473–81.
[11] Eringen AC. Linear theory of nonlocal elasticity and dispersion of plane waves. Int J Eng Sci. 1972;10(5):425–35.
[12] Eringen AC, Edelen DGB. On nonlocal elasticity. Int J Eng Sci. 1972;10:233–48.
[13] Eringen AC. On differential equations of nonlocal elasticity and solutions of screw dislocation and surface waves. J Appl Phys. 1983;54:4703–10.
[14] Shariati M, Shishehsaz M, Sahbafar H, Pourabdy M, Hosseini M. A review on stress-driven nonlocal elasticity theory. J Comput Appl Mech. 2021;52(3):535–52.
[15] Ansari R, Rouhi H. Nonlocal Flugge shell model for the axial buckling of single-walled Carbon nanotubes: An analytical approach. Int J Nano Dimens. 2015;6(5):453–62.
[16] Kananipour H. Static analysis of nanoplates based on nonlocal based on the nonlocal Kirchhoff and Mindlin plate theories using DQM. Lat Am J Solids Struct. 2014;11(10):1709–20.
[17] Srividhya S, Raghu P, Rajagopal A, Reddy JN. Nonlocal nonlinear analysis of functionally graded plates using third-order shear deformation theory. Int J Eng Sci. 2008;125:1–22.
[18] Phung-Van P, Lieu QX, Nguyen-Xuan H, Abdel Wahab M. Size-dependent isogeometric analysis of functionally graded carbon nanotube-reinforced composite nanoplates. Compos Struct. 2017;166:120–35.
[19] Thai S, Thai HT, Vo TP, Patel VI. A simple shear deformation theory for nonlocal beams. Compos Struct. 2018;183:262–70.
[20] Jape AS, Sayyad AS. Bending of functionally graded nanobeams using hyperbolic nonlocal theory. IOP Conf Ser: Mater Sci Eng. 2022;1236(1):012088.
[21] Karami B, Janghorban M, Tounsi A. Variational approach for wave dispersion in anisotropic doubly-curved nanoshells based on a new nonlocal strain gradient higher order shell theory. Thin Wall Struct. 2018;129:251–64.
[22] Arefi M, Zenkour AM. Size-dependent free vibration and dynamic analyses of piezo-electro-magnetic sandwich nanoplates resting on viscoelastic foundation. Phys B: Condens Matter. 2017;521:188–97.
[23] Mematollahi MS, Mohammadi H, Nematollahi MA. Thermal vibration analysis of nanoplates based on the higher-order nonlocal strain gradient theory by an analytical approach. Superlattices Microstruct. 2017;111:944–59.
[24] Arefi M. Analysis of doubly curved piezoelectric nano shell: Nonlocal electro-elastic bending solution. Eur J Mech A/Solids. 2018;70:226–37.
[25] Ansari R, Rouhi H, Arash B. Vibrational analysis of Double-Walled carbon nanotubes based on nonlocal Donnell shell theory *via* a new numerical approach. Iran J Sci Technol B. 2013;37:91–105.
[26] Sahmani S, Fattahi AM. Nonlocal size dependency in nonlinear instability of axially loaded exponential shear deformable FG-CNT reinforced nanoshells under heat conduction. Eur Phys J Plus. 2017;132:231.
[27] She GL, Ren YR, Yuan FG, Xiao WS. On vibrations of porous nanotubes. Int J Eng Sci. 2018;125:23–35.
[28] Şimşek M, Yurtcu HH. Analytical solutions for bending and buckling of functionally graded nanobeams based on the nonlocal Timoshenko beam theory. Compos Struct. 2013;97:378–96.
[29] Karami B, Shahsavari D, Janghorban M. A compressive analytical study on functionally graded carbon nanotubes-reinforced composite plates. Aerosp Sci Technol. 2018;82–83:499–512.
[30] Thai HT, Vo TP, Nguyen TK, Lee J. A nonlocal sinusoidal plate model for micro/nanoscale plates. Proc Inst Mech Eng C J Mech Eng Sci. 2014;228(14):2652–60.
[31] Touratier M. An efficient standard plate theory. Int J Eng Sci. 1991;29:901–16.
[32] Ansari R, Sahmani S, Arash B. Nonlocal plate model for free vibrations of single-layered graphene sheets. Phys Lett A. 2010;375:53–62.
[33] Janghorban M. Static analysis of functionally graded rectangular nanoplates based on nonlocal third order shear deformation theory. Int J Eng Appl Sci. 2016;8(2):87–100.
[34] Shahrbabaki EA. On three-dimensional nonlocal elasticity: Free vibrations of rectangular nanoplates. Eur J Mech A/Solids. 2018;71:122–33.
[35] Kulikov GM, Plotnikova SV. A method of solving three-dimensional problems of elasticity for laminated composite plates. Mech Compos Mater. 2012;48(1):15–26.
[36] Kulikov GM, Plotnikova SV. Exact geometry four-node solid-shell element for stress analysis of functionally graded shell structures *via* advanced SaS formulation. Mech Adv Mater Struct. 2018;27(12):948–64.
[37] Alibeigloo A, Emtehani A. Static and free vibration analysis of carbon nanotube-reinforced composite plate using differential quadrature method. Meccanica. 2015;50:61–76.
[38] Alibeigloo A, Liew KM. Elasticity solution of free vibration and bending behavior of functionally graded carbon nanotube-reinforced composite beam with thin piezoelectric layers using differential quadrature method. Int J Appl Mech. 2015;7(1):1550002.
[39] Brischetto S. Exact three-dimensional static analysis of single- and multi-layered plates and shells. Compos B: Eng. 2017;119:230–52.
[40] Brischetto S. A 3D layer-wise model for the correct imposition of transverse shear/normal load conditions in FGM shells. Int J Mech Sci. 2018;136:50–66.
[41] Wu CP, Lu YC. A modified Pagano method for the 3D dynamic response of functionally graded magneto-electro-elastic plates. Compos Struct. 2009;90:363–72.
[42] Wu CP, Tsai YH. Static behavior of functionally graded magneto-electro-elastic shell under electric displacement and magnetic flux. Int J Eng Sci. 2007;45:744–69.
[43] Demirbaș MD. Thermal stress analysis of functionally graded plates with temperature-dependent material properties using theory of elasticity. Compos B: Eng. 2017;131:100–24.
[44] Wu CP, Chiu KH, Jiang RY. A meshless collocation method for the coupled analysis of functionally graded piezo-thermo-elastic shells and plates under thermal loads. Int J Eng Sci. 2012;56:29–48.
[45] Ferreira AJM, Roque CMC, Carrera E, Cinefra M, Polit O. Bending and Vibration of laminated plates by a layerwise formulation and collocation with radial basis functions. Mech Adv Mater Struct. 2013;20(8):624–37.
[46] Kulikov GM, Plotnikova SV. Strong sampling surfaces formulation for layered shells. Int J Solids Struct. 2017;121:75–85.
[47] Kulikov GM, Plotnikova SV. Strong sampling surfaces formulation for laminated composites plates. Compos Struct. 2017;172:73–82.

[48] Wei GW. Discrete singular convolution for beam analysis. Eng Struct. 2001;23(9):1045–53.
[49] Civalek Ö, Gürses M. Discrete singular convolution for free vibration analysis annular membranes. Math Comput Appl. 2009;14(2):131–8.
[50] Wang X. Differential quadrature and differential quadrature based element methods. Waltham, UK: Butterworth-Heinemann; 2015.
[51] Bellman R, Casti J. Differential quadrature and long-term integration. J Math Anal Appl. 1971;34(2):235–8.
[52] Bert CW, Malik M. Differential quadrature method in computational mechanics: A review. Appl Mech Rev. 1996;49(1):1–28.
[53] Flügge W. Stresses in shells. Berlin: Springer-Verlag; 1960.
[54] Leissa AW. Vibrations of shells. Washington: NASA Sp. 288; 1973.
[55] Gould PL. Analysis of shells and plates. New York (NY), USA: Springer-Verlag; 1988.
[56] Soedel W. Vibrations of shells and plates. New York (NY), USA: Marcell Dekker; 2004.
[57] Wu CP, Li WC. Three-dimensional static analysis of nanoplates and graphene sheets by using Eringen' s nonlocal elasticity theory and the perturbation method. Comput Mater Contin. 2016;52(2):73–103.
[58] Monge JC, Mantari JL. 3D elasticity numerical solution for the static behavior of FGM shells. Eng Struct. 2020;110159.
[59] Monge JC, Mantari JL, Arciniega RA. Computational semi-analytical method for 3D elasticity bending solution of laminated composite and sandwich doubly-curved shells. Eng Struct. 2020;221:110938.
[60] Brischetto S, Tornabene F. Advanced GDQ models and 3D stress recovery in multilayered plates, spherical and double-curved panels subjected to transverse shear loads. Compos B: Eng. 2018;146:244–69.
[61] Tornabene F, Brischetto S. 3D capability of refined GDQ models for the bending analysis of composite and sandwich plates, spherical and doubly curved shells. Thin Wall Struct. 2018;129:94–124.
[62] Tornabene F, Fantuzzi N, Ubertini F, Viola E. Strong formulation finite element based on differential quadrature: A survey. Appl Mech Rev. 2015;67(2):1–55.
[63] Shu C. Differential Quadrature and its application in engineering. London, UK: Springer; 2000.
[64] Nguyen NT, Hui D, Lee J, Nguyen-Xuan N. An efficient computational approach for size-dependent analysis of functionally graded nanoplates. Comput Methods Appl Mech Eng. 2015;297:191–218.
[65] Mori T, Tanaka K. Average stress in matrix and average elastic energy of materials with misfitting inclusions. Acta Metall. 1973;21:571–4.
[66] Tornabene F, Fantuzzi N, Bacciocchi M, Viola E. Effect of agglomeration on the natural frequencies of functionally graded carbon nanotube-reinforced laminated composite doubly-curved shells. Compos B: Eng. 2016;89:187–218.
[67] Arefi M, Kiani Moghaddam S, Mohammad-Rezaei Bidgoli E, Kiani M, Civalek O. Analysis of graphene nanoplatelet reinforced cylindrical shell subjected to thermo-mechanical loads. Compos Struct. 2021;255:112924.